DOI 10.1002/pmic.201100556 *Proteomics* 2012, *12*, 1194–1206

RESEARCH ARTICLE

Protein turnover: Measurement of proteome dynamics by whole animal metabolic labelling with stable isotope labelled amino acids

Amy J. Claydon[1], Michael D. Thom[2], Jane L. Hurst[2] and Robert J. Beynon[1]

[1] Protein Function Group, Institute of Integrative Biology, University of Liverpool, Liverpool, UK
[2] Mammalian Behaviour and Evolution Group, Institute of Integrative Biology, University of Liverpool, Leahurst Campus, Neston, UK

The measurement of protein turnover in tissues of intact animals is obtained by whole animal dynamic labelling studies, requiring dietary administration of precursor label. It is difficult to obtain full labelling of precursor amino acids in the diet and if partial labelling is used, calculation of the rate of turnover of each protein requires knowledge of the precursor relative isotope abundance (RIA). We describe an approach to dynamic labelling of proteins in the mouse with a commercial diet supplemented with a pure, deuterated essential amino acid. The pattern of isotopomer labelling can be used to recover the precursor RIA, and sampling of urinary secreted proteins can monitor the development of liver precursor RIA non-invasively. Time-series analysis of the labelling trajectories for individual proteins allows accurate determination of the first order rate constant for degradation. The acquisition of this parameter over multiple proteins permits turnover profiling of cellular proteins and comparisons of different tissues. The median rate of degradation of muscle protein is considerably lower than liver or kidney, with heart occupying an intermediate position.

Received: October 21, 2011
Revised: November 26, 2011
Accepted: November 28, 2011

Keywords:
Animal proteomics / Precursor pool / Protein turnover / Stable isotope labelling

1 Introduction

Since the pioneering work of Schoenheimer et al. [1], it has been recognized that proteins in the cell are in a dynamic state of turnover, and that the rate of turnover and imbalance between synthesis and degradation can lead to changes in the expressed profile in the cell. Proteins within a cell or tissue can share similar rates of synthesis, and have a comparable abundance of mRNA, but differences in their rates of degradation are responsible for differences in the steady state concentration of each protein. Early studies on protein turnover were constrained by low levels of incorporation of radiolabelled amino acids, such that it was challenging to work with single proteins, and, more commonly, 'total protein' turnover was assessed. A proteomics perspective would require determination of the turnover rates of individual proteins in a proteome and the central role of mass spectrometry (MS) indicates the possibility of determination of the rate of incorporation of stable isotope metabolic label into proteins, or conversely, the rate of loss of label from pre-labelled proteins (these are formally and analytically equivalent, but technical considerations can pre-dispose the experiment towards one approach or the other). The precursors can be simple metabolic precursors (such as [^{13}C]glucose [2] [$^{2}H_2$]O [3–6], stable isotope labelled amino acids [7–17], or uniformly [^{15}N]-labelled diets [10, 18, 19]. In some labelling protocols, the incorporation of label into proteins can result in complex isotope labelled patterns, although there are emergent software solutions that ease the analysis of the complex isotope profiles [18, 20–23].

The simplest proteome turnover study is delivered in isolated cells (prokaryote or eukaryote) maintained in minimal

Correspondence: Professor Rob Beynon, Protein Function Group, Institute of Integrative Biology, University of Liverpool, Crown Street, Liverpool L69 7ZB, UK
E-mail: r.beynon@liv.ac.uk

Abbreviations: MUP, major urinary protein; **RIA**, relative isotope abundance

Colour online: See the article online to view Figs. 1–3, 5–7 and 10 in colour.

media, such that a single amino acid (such as [$^{13}C_6$]arginine or [$^{2}H_{10}$]leucine) can be delivered in either fully labelled or unlabelled form (e.g. [8, 17]). The particular advantage of this experimental system is that it allows the relative isotope abundance (RIA) of the label to be set at unity and zero (or vice versa, depending on whether an 'unlabelling' or a labelling protocol is chosen). The size of the pool of amino acid, or other label, in the medium is substantially larger than the intracellular pool, and thus, the precursor pool is rapidly equilibrated and reaches that of the medium pool very quickly. As a protein is completely turned over (replaced) it undergoes a transition between label-free and fully labelled forms, maximizing the dynamic range of the transition that can be recovered [8, 11, 17]. In more complex systems, such as animals, it is more difficult to establish similar turnover studies. First, there can be no instantaneous shift to a completely labelled precursor pool, as there will be substantial biomass in the animal tissues contributing to the precursor pool. Second, over extended periods, the only feasible route of administration of the label is in drinking water [3, 4, 24] or the diet, which introduces the complexity of meal feeding (e.g. during the active, dark part of the diurnal rhythm for rodents). The small intestine and the liver (via the portal delivery from the gut) are most exposed to this variation in dietary input, whereas other tissues are more metabolically remote and dampen such variance. The uncertainty over the processing of input label means that it is important to assess the degree of labelling of the precursor pool, most simply expressed as the precursor RIA.

For labelling with single amino acids, the route to recovery of the precursor RIA is via peptides that contain at least two instances of that amino acid. If, for example [$^{13}C_6$]lysine or [$^{13}C_6$]arginine were used as label, then very few doubly labelled peptides would be obtained from a tryptic digest (peptides containing R-P or K-P, or miscleaved peptides being the exception). However, calculation of the precursor RIA does not have to be conducted in the same experiment as the determination of turnover rates, and proteases of different specificity could also be used to generate multiply labelled peptides. The alternative approach is to use a labelled amino acid that is not bound to the primary specificity of the protease that is being used. For example, leucine and valine are abundant amino acids in the proteome and have the added advantage that because they are essential amino acids, there can be no contribution from endogenous amino acid biosynthesis by the animal.

The aim of this experiment was to label newly synthesized proteins in the mouse through the supplementation of stable isotope labelled (heavy) valine into a standard mouse diet. Valine was chosen as an abundant amino acid in the proteome, increasing the probability of readily analysable, labelled peptides. Dietary administration of labelled amino acids does not lead to an artificial increase in protein synthesis, as has been reported with intravenously infused amino acids [25]. Preparation of a diet in which all valine was stable isotope labelled would be complex, and would require a totally synthetic diet – this is substantially more complex than diets containing uniformly [^{15}N]-labelled bacteria or algae, for example. Totally synthetic diets are unpalatable in chickens, for example, and could result in a reduced food intake [15, 16]. Finally, diets prepared with [^{13}C]-labelled amino acids in synthetic rodent diets are expensive. In this study, we explored the feasibility of measurement of protein turnover rates using a diet comprising a standard laboratory diet supplemented with a labelled amino acid. Moreover, we assessed the feasibility of using a uniformly deuterated amino acid ([$^{2}H_8$]valine) as an affordable option. Because the diet was supplemented with a crystalline amino acid, but was otherwise unchanged, we did not anticipate any complication of palatability or well-being of the animals. However, the dilution of the labelled precursor by unlabelled amino acids in the diet, as well as the existing tissue reserves of valine meant that the RIA would not be known [15], although it was designed to be 0.5 in the dietary preparation.

In our previous studies on birds [16], tissue samples were taken at regular intervals during the labelling period to monitor the rise to plateau of the RIA of the tissue precursor pools. This required a large number of animals (42 chicks over 5 days). However, mice and rats both exhibit an obligate proteinuria in the form of major urinary proteins (MUPs). MUPs are lipocalins intimately associated with chemical communication between individuals [26–32]. They are encoded by a multigene family on chromosome 4 and many of these genes are transcribed and translated in the liver and constitutively output into the urine via plasma. We surmised that analysis of the labelling trajectory of the MUPs would report directly on the precursor RIA in liver and thus, could be used to assess dietary incorporation into the animal at a high frequency of sampling that would be non-invasive, requiring straightforward urine sampling.

2 Materials and methods

2.1 Experimental animals

Fifteen hybrid male laboratory mice, heterozygous for MUP type B6/BALBc (C57BL/6JOlaHsd × BALB/cOlaHsd), provided all urine and tissue samples. They were housed individually in polypropylene cages containing sawdust substrate and shredded paper for nesting material. As stress can affect food intake and, potentially, protein metabolism, the mice were kept in an environment with no stressors, that is housed at ambient temperature (19–23°C) and humidity (50–60%) under 12-h light:dark reverse lighting, with white light from 8 p.m. to 8 a.m. Urine samples were collected from different animals at approximately 2-h intervals during the dark phase, under dim red lights, when the mice were most active. Urine was collected by gentle restraint at the scruff of the neck, and mice were held over a micro-centrifuge tube; if a sample was not voluntarily released the bladder was massaged lightly. The overall workflow is summarized in Fig. 1.

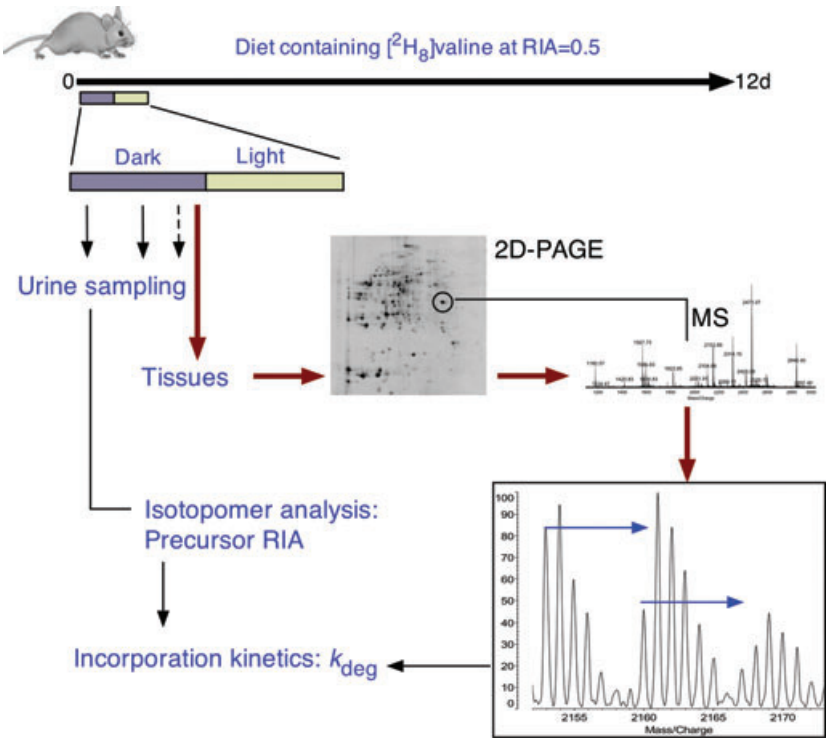

Figure 1. Experimental workflow for turnover studies. A standard laboratory diet was supplemented with crystalline [$^2H_8$]valine such that the precursor RIA would be 0.5. Animals were acclimated to the same diet supplemented with unlabelled valine prior to transfer to the labelled diet. Between 2 and 12 days after introduction of the new diet, animals were killed and tissues recovered for proteome analysis. Urine samples were collected at frequent intervals from all animals for analysis of labelling patterns in the MUPs.

Two different diets were produced for these studies, both based on the 5002 Certified Rodent Diet (LabDiet®, Purina Test Diet, PMI, MO, USA), which is pelleted and contains 20% (w/w) protein, of this 1.05% (w/w) is natural valine, predominantly incorporated into protein. When the labelled and unlabelled diets were prepared (by International Product Supplies, London), supplementary crystalline valine, also at 1.05% (w/w), unlabelled or in the form of [$^2H_8$]valine (Cambridge Isotopes) was included. The unlabelled semi-synthetic diet was prepared to acclimate the animals to the diet before introduction of the labelled diet. During the acclimation phase, the weights of the mice and food were monitored to assess eating, the health of the mice was also closely monitored. During both acclimation and labelling phases of the experiment, food and water were provided ad libitum.

2.2 Sample preparation, urine

All urine samples were stored at −20°C within 15 min of collection until analysis. After steps to reduce and alkylate disulphide bridges in the MUPs, the urine was proteolysed with endopeptidase LysC. Initially samples were diluted 1:100 into water, 30 μL of this dilution (approximately 6 μg protein) was added to 30 μL 20 mM DTT in 50 mM ammonium bicarbonate and incubated at 56°C for 20 min. Samples were cooled before addition of 60 μL 100 mM iodoacetamide (IAA) in 50 mM ammonium bicarbonate buffer. This was again incubated for 30 min prior to addition of 5 × volume of ice cold 30% trichloroacetic acid (TCA) for protein precipitation. Samples were centrifuged at 15 000 × *g* for 5 min to pellet the proteins, the TCA was then removed and pellets were washed three times with excess diethyl ether. After evaporation of the solvent, pellets were resuspended in 10 μL 25 mM ammonium bicarbonate and digested overnight with 0.1 μg endopeptidase LysC.

2.3 Sample preparation, tissues

At 4 p.m. on each sampling day, liver, heart and kidneys from two mice (one mouse on day 10) were washed with phosphate buffered saline, pH 7.5, to remove the majority of residual blood. Skeletal muscle was also taken from the hind limb and washed with phosphate buffered saline. Samples were kept on dry ice until transfer to a freezer at −20°C for storage. All tissue samples were weighed and homogenized, using a Polytron homogenizer at 100 mg tissue per mL of 20 mM phosphate buffer, pH 7.5, in the presence of protease inhibitors (complete protease inhibitors, Roche Diagnostics). The resulting homogenate was centrifuged at 4°C for 45 min at 15 000 × *g* and the supernatant fraction was recovered and stored at −20°C.

2.4 2D gel electrophoresis

Samples were separated by 2D SDS-PAGE using 13 cm immobilized pH gradient (IPG) strips, pH 3–10. The proteins

present on the gel, after Coomassie blue staining, were subject to in-gel tryptic digestion; 1 mm^2 segments of gel were excised from stained protein spots and destained in 1:1 ACN: 50 mM ammonium bicarbonate buffer. Samples were reduced with 10 mM DTT and alkylated with 55 mM IAA to prevent disulphide bridges reforming. The gel plug was dehydrated in ACN, rehydrated in 25 mM ammonium bicarbonate buffer and exposed to proteolytic digestion with trypsin overnight at 37°C. Using MALDI-TOF MS, the protein present in each band was identified using peptide mass fingerprinting in conjunction with database searches using Mascot against SwissProt, *Mus* taxonomy, and the peak intensities of valine containing peptides were recorded.

2.5 MALDI-TOF MS

Peptide mass spectra were acquired using a Shimadzu-Biotech Axima MALDI-TOF^2 mass spectrometer, in positive ion reflectron mode, using automated data acquisition. The matrix was CHCA at 7 mg/mL in 50% ACN, 0.1% TFA. A calibration well was incorporated into the automated acquisition at regular intervals to re-calibrate the instrument during data collection. Data were processed using Shimadzu-Biotech Launchpad (version 2.7) software.

2.6 Calculation of precursor RIA

The RIA of the amino acid precursor pool dictates the probability that a heavy or light valine amino acid is incorporated into new proteins during translation. The distribution of [$^2H_8$]valine in the urinary proteins was used to calculate the RIA of [$^2H_8$]valine in the amino acid precursor pool of the liver, using mass isotopomer distribution analysis (MIDA) [6]. To be informative, peptides must contain at least two instances of the stable isotope labelled residue [14–16]. Two di-valine peptides were used in this analysis; FHTVRDEECSELSMVADK ([M+H]$^+$ 2152.95 m/z) and IEDNGNFRLFLEQIHVLENSLVLK ([M+H]$^+$ 2840.51 m/z). In brief, for a di-valine peptide there are two possible positions for incorporation of the heavy valine residue (H) and from these, there are three possible peaks on a mass spectrum corresponding to two light valine residues (LL), one light and one heavy (LH and HL) and two heavy valine residues (HH). If the RIA of the valine is *r*, then the RIA of the light variant is $(1 - r)$. So, the probability of an all-heavy di-valine peptide is r^2 and an all-lightpeptide would be $(1 - r)^2$. The intensity of the HL peptide is represented by $2(r \times (1 - r))$ (the multiplier of two is required to allow for the two positional variants). Thus, the ratio of the intensities of the HH and HL peptides is as follows:

$$\frac{I_{HH}}{I_{HL}} = \frac{r^2}{2 \cdot r(1-r)} = \frac{r}{2 \cdot (1-r)}$$

and thus, knowing the intensity ratio of HH and HL(x) permits the value of r, the precursor RIA, to be calculated:

$$r = \frac{2x}{1+2x}$$

Once a value for the RIA of the precursor pool is established, the rate of turnover for individual proteins can be calculated. Mono-valine peptides are used for analysis of individual protein turnover and the ratio of the heavy and light peaks is calculated using the intensities (I) of the heavy and light peptides; $RIA_t = I_H/(I_H + I_L)$. If these values are plotted against time it is possible to recover the rate of turnover (expressed as the fractional first order rate constant for replacement, k) for each protein using the equation:

$$RIA_t = RIA_\infty \cdot (1 - e^{-kt})$$

where RIA_∞ is set as a fixed value for each tissue and k is the first order rate constant defining the rate of replacement (turnover) of the protein.

The extent of transamination of the [$^2H_8$]valine (leading to loss of the α-carbon deuteron) was assessed by non-linear optimization of the summed overlapping spectra for a theoretical mixture of the [$^2H_8$] and [$^2H_7$] peptides, compared to the observed intensities of the overlapping profiles of the two peptide variants in the mass spectrum. The theoretical spectra were obtained from the MS-Isotope tool (http://prospector.ucsf.edu/). The theoretical and experimental spectra were fitted using the non-linear optimizer within Excel, using the summed squares of residuals for ion intensities and thus yielding the fraction of labelled valine that had been transaminated.

3 Results and discussion

In a steady state the only method to assess the dynamic state of individual proteins is to monitor the movement of a tracer through the protein pool. We fed mice a standard laboratory diet that had been formulated to contain [$^2H_8$]valine at a level equivalent to the amount of protein-bound valine in the diet. Animals were acclimated to the diet containing free valine in the unlabelled form before transfer to the labelled diet; throughout the entire period there was no significant change in body weight of the mice and food consumption was unaltered (data not shown). At times over a 12-day labelling period, four tissues (liver, kidney, heart and skeletal muscle) were analysed by MS for the pattern of incorporation of label into individual proteins that were resolved on 2D-PAGE and analysed by MALDI-TOF MS (Fig. 1). The abundance of valine in the mouse proteome is slightly less than 1 in 20 (4.6%) and thus multiple tryptic peptides would be expected in any proteome analysis. To illustrate, we analysed the mouse liver and muscle proteome samples by LC-MS/MS using an Orbitrap Velos (results not shown). For liver, 11, 356 peptides yielded 56% containing valine and of this subset, 64% contained a

mono-valine residue, 25% were di-valine peptides and 11% contained three or more valine residues. For muscle, the data were similar: 57% of analysable peptides contained valine residues, of which 59% contained one valine residues, 27% were di-valine peptides and 14% contained three or more valine residues. Thus, approximately half of all peptides contained a valine residue and a large majority of proteins would be expected to yield turnover data.

We expected that the labelled valine would be absorbed rapidly across the small intestine and enter the portal circulation where it would be absorbed by the liver. To monitor the availability of labelled valine for hepatic protein synthesis, we analysed the incorporation of labelled amino acid in proteins that are secreted from the liver, as these proteins represent an instantaneous sample of the amino acid pool available for hepatic protein synthesis. Newly synthesized plasma proteins enter the pool of pre-existing proteins, and thus, the extent of labelling is apparently lower than for proteins that are lost irreversibly from the animal. Hence, we used MUPs to access the liver synthetic process. MUPs are products of a polymorphic gene cluster and are present at high concentrations in urine (typically 10–20 mg/mL) where they evince complex roles in chemical communication between individuals [26–32]. Urine samples were collected at regular intervals during the active (dark) period from mice fed on a diet containing stable isotope labelled valine. As the mice entered the experiment with no labelled valine present, a general shift from light to heavy proteins would be expected as the label is incorporated into new protein. Proteolysis of the urine with endopeptidase LysC revealed both mono- and di-valine peptides that contained labelled valine. The data from the urinary proteins do not give meaningful turnover values for MUPs as they are instantly transported from the liver after synthesis and do not degrade until they are deposited in the environment. They do however give daily temporal sampling of the RIA of the amino acid precursor pool of the liver, which lends itself to the analysis of liver precursor pool behaviour without the need to take regular tissue samples.

Determination of the RIA of the precursor pool requires the analysis of peptides that contain at least two valine residues. Digestion with endopeptidase LysC [28] generated peptides with multiple instances of valine, some of which yielded strong ion signals upon MALDI-TOF analysis (Fig. 2). Although the two peptides illustrated in Fig. 2 are very similar in sequence, they were derived from different MUPs, and are different in mass because of a polymorphism that generated an endopeptidase LysC site. A minor but tractable complication derived from the partial transamination of [$^2H_8$]valine in the tissue (see later) was managed by measurement of the incorporation of both forms of the amino acid. Once this was taken into account, the resultant RIA value was reliable. Analysis of di-valine MUP peptides from the LysC digests of urine reveal that the liver precursor pool reaches a high extent of labelling 10 h after the labelled diet was introduced to the mice (Fig. 2), indicating a very rapid internal turnover and utilization of ingested amino acids.

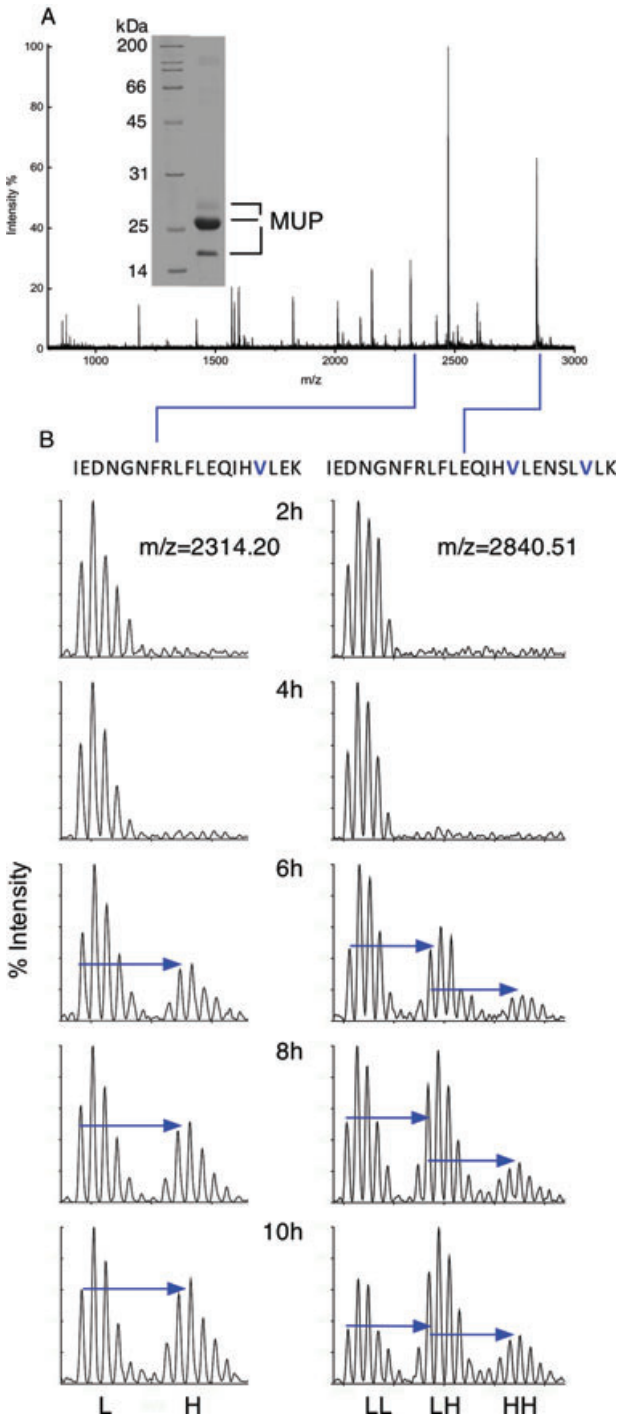

Figure 2. Non-invasive determination of precursor labelling by analysis of MUPs. MUPs are high abundant proteins in mouse urine (inset SDS-PAGE image). Digestion of abundant MUPs with trypsin elicited very few di-valine peptides (not shown), and digestion with a protease of increased specificity (endopeptidase LysC) was required to generate informative di- or tri-valine peptides (A). Urinary MUPs were recovered over the first 10 h (dark period) of dietary administration, and the incorporation of heavy valine was monitored by MALDI-TOF MS (B). Representative isotope incorporation profiles are given for a mono-valine peptide (IEDNGNFRLFLEQIHVLEK ([M + H]$^+$ 2314.20 *m/z*) and a di-valine peptide IEDNGNFRLFLEQIH**V**LENSL**V**LK ([M + H]$^+$ 2840.5] *m/z*).

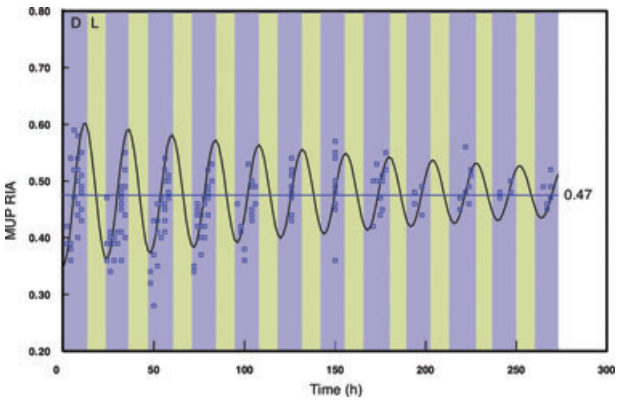

Figure 3. Time dependence of precursor RIA pool in liver. The RIA of valine in the liver was assessed by serial sampling of MUPs at different times during the dark period (shaded segments 'D') on each of 12 successive days (because some animals were killed on each day, the sample number declined over time). The MUPs were digested with endopeptidase LysC and the precursor RIA value was calculated for individual MUP samples using di-valine peptides. The solid line is a sinusoidal function, the periodicity of which is 24 h with an exponentially decaying amplitude (see text).

Urine sampling is non-invasive and it was possible to obtain repeated samples from individuals throughout the labelling period. In total, 179 urine samples were collected over the 12-day labelling period and the MUPs were digested with endopeptidase LysC then analysed by MALDI-TOF MS. At this high frequency of sampling, it was evident that there was a discernible oscillation in the precursor RIA (Fig. 3). During the first dark, active period (during which the animals are feeding), the precursor RIA rose to values higher than the anticipated input valine RIA (0.5), and subsequently, during the inactive, light period, the RIA fell to values below 0.5. Exploration of this oscillation revealed a pattern that could be described as a damped sinusoidal curve (Fig. 3). This curve had a periodicity of 24 h, and oscillated around an RIA 0.47. The amplitude of the excursion started at 0.14 and declined over time with an exponential rate constant of 0.005/h. We do not ascribe great significance to the parameters of this line, although the behaviour is in complete accord with what might be anticipated. It is probable that during the early phase of the feeding period, the free [$^2H_8$]valine was preferentially absorbed, leading to an overshoot in apparent RIA. Then, as the unlabelled proteins in the diet were absorbed, the enrichment of the precursor pool declined, initially to below the expected RIA, as the pool adjusted to preferential enrichment in unlabelled amino acids. Over the labelling experiment, these oscillations declined as the precursor pool gradually equilibrated with tissue amino acids and proteins, leading to a buffering of the variation. This behaviour would be a feature of all meal-feeding regimens, and illustrates the value of urinary MUP sampling to discern the high frequency components of the precursor pool behaviour. Tissues would

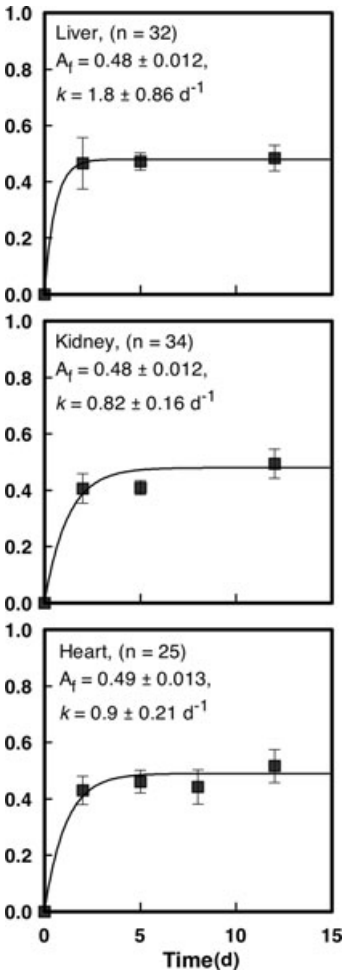

Figure 4. Precursor RIA analysis for three different mouse tissues. For three tissues (liver, kidney, heart), the trajectory of the precursor RIA was obtained by analysis of di-valine peptides from multiple proteins. The proteins and peptides used in this analysis were as follows: liver: 78 kDa glucose-regulated protein (KSDIDEIVLVGGSTR), arginase-1 (STVNTAVALTLACFGTQR), regucalcin (WDTVSNQVQR), carbonic anhydrase 3 (VVFDDTYDR), fructose-1,6-bisphosphatase 1 (SSYATCVLVSEENTNAIIIEPEKR); kidney: delta-1-pyrroline-5-carboxylate dehydrogenase (STGSVVGQQPFGGAR), alpha-enolase (AGYTDQVVIGMDVAASEFYR), aldehyde dehydrogenase (TFVQENVYDEFVER), phosphatidylethanolamine-binding protein 1 (GNDISSGTVLSDYVGSGPPSGTGLHR), sorbitol dehydrogenase (TLNVKPLVTHRFPLEK), peptidyl-prolyl cis-trans isomerase A (VNPTVFFDITADDEPLGR), heat shock cognate 71 kDa protein (QTQTFTTYSDNQPGVLIQVYEGER), actin cytoplasmic 2 (AVFPSIVGRPR), alcohol dehydrogenase (AVPREELFVTSK); heart: ATP synthase subunit beta (WVVIGDENYGEGSSR), creatine kinase (SFLVWVNEEDHLR), malate dehydrogenase (IFGVTTLDIVR), triosephosphate isomerase (DLGATWVVLGHSER), ETF subunit beta (GIHVEIPGAQAESLGPLQVAR), phosphatidylethanolamine-binding protein 1 (GNDISSGTVLSDYVGSGPPSGTGLHR), fatty acid-binding protein, heart (LILTLTHGSVVSTR), delta(3,5)-delta(2,4)-dienoyl-CoA isomerase (VIGNQSLVNELTFSAR), heat shock protein 70 cognate (NQVAMNPTNTVFDAK). Symbols define the mean (± SD, n variable) value of the calculated RIA for each time point and the line is the fitted mono-exponential curve.

be expected to dampen such oscillations, particularly as they become metabolically and physically remote from the portal input (post-hepatic) and notwithstanding the oscillatory component, the precursor and protein RIA values can nonetheless be analysed by simple exponential curves (see later). Indeed, any attempt to superimpose the diurnal rhythm on this exponential process would be pointless, as it would require very high frequency tissue sampling (and thus, many more animals) to preclude aliasing effects and would not be justified on ethical or cost grounds. Nonetheless, the value of urinary protein sampling to determine high frequency liver labelling dynamics is evident.

For three tissues (liver, kidney and heart), the rate of protein labelling was sufficiently high that the trajectory of the precursor RIA could be assessed over the entire labelling period by analysis of di-valine peptides from multiple proteins and peptides (Fig. 4). For skeletal muscle, the rate of turnover of protein was so low that significant label incorporation was not evident at early time points, and it was not possible to acquire data to define the (RIA, *t*) curve for this tissue. In the three tissues for which data were acquired, the plateau RIA was attained after approximately 2 days of labelling and was maintained for the remainder of the experiment. In all instances, the plateau RIA value was between 0.48 and 0.49, consistent with effective delivery of the valine pool to tissues and efficient utilization of both free and protein bound amino acids in the ingesta. When the liver pool was analysed via the MUPs, the plateau RIA was 0.47 (results not shown).

To assess the turnover rate of individual proteins, soluble protein preparations for four different tissues (liver, kidney, heart and skeletal muscle) were separated by 2D gel electrophoresis for each of two animals at four different times (days 1, 2, 5 and 12) during the labelling experiment; a total of 32 gels (Fig. 5). On each gel, the same spot was then excised, subject to in-gel digestion and the resultant peptides were analysed by MALDI–TOF MS to obtain the identity of the protein by peptide mass fingerprinting. Further, the pattern of labelling of mono-valine peptides was analysed to acquire the rate of turnover of each protein – the spots corresponding to the same proteins on each gel were analysed for each time point and for each of the duplicate animals. Although many proteins were identified, only those containing a readily analysable mono-valine peptide are included here. The ratio of peak intensities for mono-valine peptides, taken as $RIA_t = I_H/(I_H + I_L)$, were plotted against time for each protein (Fig. 6) and analysed by non-linear curve fitting to derive the first order rate constant for turnover. The second parameter, the value of RIA at plateau (RIA_∞), was set as a constant value corresponding to the plateau RIA calculated for the tissue precursor pool. For liver, this value was (±SEM), 0.48 ± 0.012; for kidney, 0.48 ± 0.012 and for heart, 0.49 ± 0.013. Accurate determination of the precursor plateau RIA for skeletal muscle by curve fitting of the labelling trajectory was difficult because of the low rate of label incorporation into proteins from this tissue and we have assumed a value of 0.48 for this tissue, taken as the average of day 12 precursor RIA values for this tissue. Turnover data were obtained for a total of 127 proteins over the four tissues (Supporting Information Table S1). The error (SEM/rate constant × 100) in the fitted value of *k* was liver: 11.4%, kidney: 10.3%, heart: 16.6% and skeletal muscle: 24%. The higher uncertainty in heart and skeletal muscle parameters was probably due to the lower rate of turnover of proteins in these tissues, making determination of the degree of labelling more challenging at early time points. Rather than plot the individual labelling curves for each protein in individual graphs (these are presented in Supporting Information Fig. S1), we have profiled the turnover characteristics of each tissue by plotting the turnover trajectory for each protein based on the fitted parameters (Fig. 6). To define turnover, we calculate and report the first order rate constant for degradation, k_{deg}, as this is the linear parameter, and analysis of protein half life ($= \ln(2)/k_{deg}$), although conceptually simpler, can lead to misinterpretation of data as it is a reciprocal transformation. The distribution of k_{deg} values was not normal (Shapiro–Wilk test, alpha = 0.01, $p < 0.006$ in all four instances), and a non-parametric display of the turnover values emphasized the tissue differences (Fig. 7). From these profiles, it is immediately evident that liver and kidney (median k_{deg} of 0.162/day and 0.156/day, respectively) have a higher rate of protein turnover than cardiac muscle (median $k_{deg} = 0.059$/day), which in turn has a higher rate of turnover than skeletal muscle (median $k_{deg} = 0.023$/day).

The intrinsic differences in median degradation rate could be attributable to changes in the activity of the degradative machinery in individual tissues, affecting all proteins equally. Alternatively proteins might have an intrinsically altered rate of degradation. For a limited subgroup of proteins, it was possible to derive the rate of turnover for the same protein from each of two tissues (Fig. 8). In a comparison of liver and kidney, data were obtained for 14 proteins (Fig. 8A). Overall, the relationship between degradation rate in the two tissues was remarkably consistent, and only two proteins (isocitrate dehydrogenase and catalase) demonstrated a notable tissue specific rate of turnover. Isocitrate dehydrogenase (IDHC_MOUSE, O88844) was turned over approximately twice as rapidly in kidney, and by contrast, catalase was degraded three times more rapidly in liver. Isocitrate dehydrogenases are enzymes involved in the conversion of isocitrate to α-ketoglutarate in the citric acid cycle. An additional function of the cytoplasmic $NADP^+$-dependent isocitrate dehydrogenase is the formation of NADPH critical to the reduction of glutathione. The liver is responsible for detoxification and glutathione conjugation; therefore, the demand for isocitrate dehydrogenase [NADP] might be constant, obviating a high rate of turnover. By contrast, in the kidney, isocitrate dehydrogenase [NADP] is mainly required during stress or injury and a higher rate of turnover would allow this enzyme to be produced and removed as appropriate [33, 34]. The disparity between the rate of turnover of catalase (CATA_MOUSE, P24270) in the liver and kidneys is not readily explicable, but the protein is considerably less stable in liver. These two

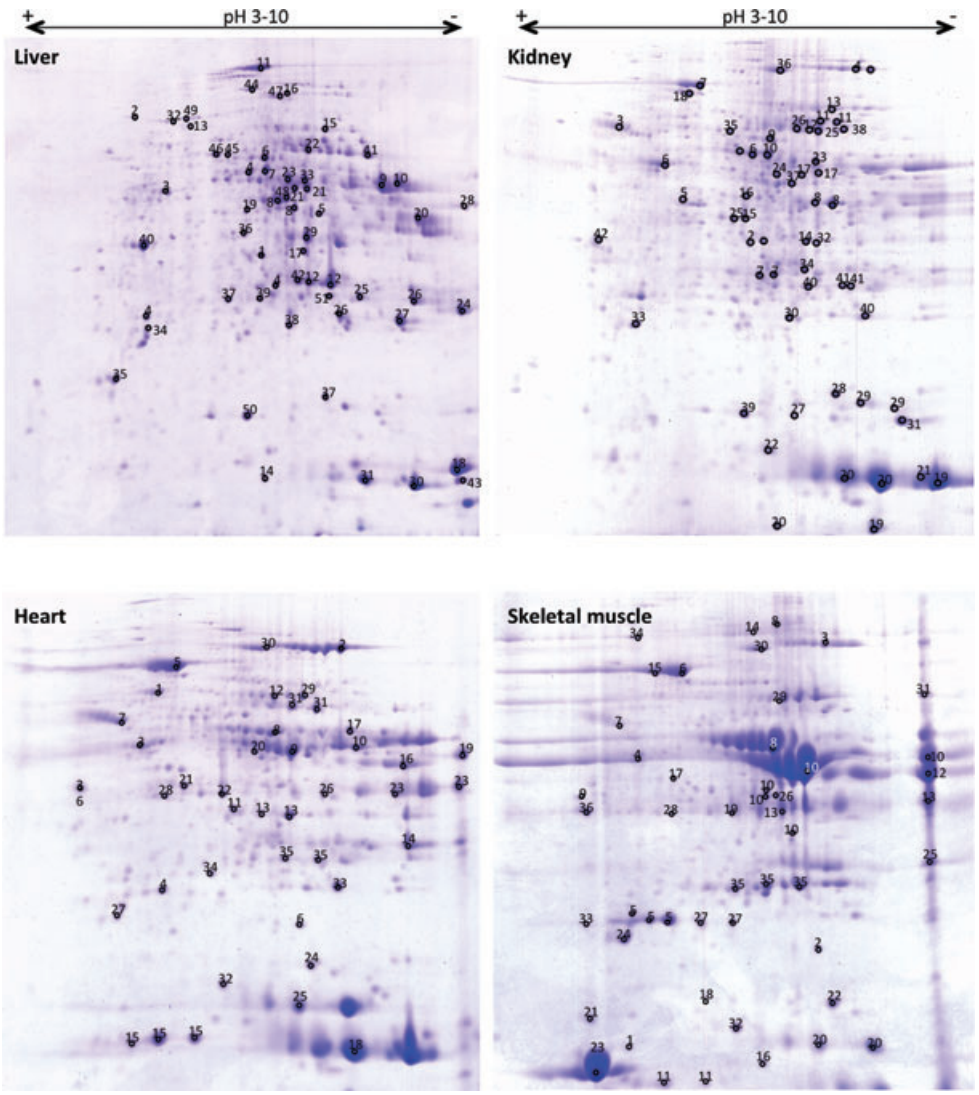

Figure 5. 2D-PAGE of soluble proteins from four mouse tissues. Four tissues (liver, kidney, heart and skeletal muscle) were analysed by 2D-PAGE. From each tissue, the most abundant spots (numbered) were harvested and subjected to in-gel digestion and MALDI-TOF MS, at each of four time points and for duplicate animals at each time point. From the isotopic labelling pattern of high intensity mono-valine peptides, turnover parameters were obtained.

exceptions aside, the consistency of protein turnover rates between liver and kidney served to contrast with and emphasize the rather remarkable differences for 14 proteins in heart and skeletal muscle (Fig. 8B). For almost all proteins, the rate of turnover was over five times higher in cardiac compared to skeletal muscle. Indeed the extent of label incorporation into skeletal muscle over the 12 days of the experiment was rather restricted, and complete definition of the labelling trajectories for skeletal muscle proteins would require extended labelling periods of perhaps 30–40 days. Conversely, at these times, the high turnover proteins in liver and kidney would have reached near-plateau labelling, and it would not be possible to obtain turnover rates unless earlier time points were also sampled. The analysis of tissue specific protein turnover requires carefully designed experiments that sample at times commensurate with both high and low turnover proteins.

For two proteins, malate dehydrogenase C (MDHC_MOUSE, P14152) and nucleotide diphosphate kinase B (NDKB_MOUSE, Q01768), degradation rate constants were acquired for all four tissues, and were, in the order liver, kidney, heart, skeletal muscle: MDHC: 0.15/day, 0.15/day, 0.06/day, 0.02/day, and NDKB: 0.14/day, 0.16/day, 0.07/day, 0.02/day. These data, for the same protein expressed in four different tissues, serves to emphasize that the degradative environment might be the primary determinant of the overall rate of degradation. Intracellular protein (ICP) degradation can be conceptually divided into a commitment phase and a completion phase, the former being, for example, sequestration into the lysosome or polyubiquitination, the latter

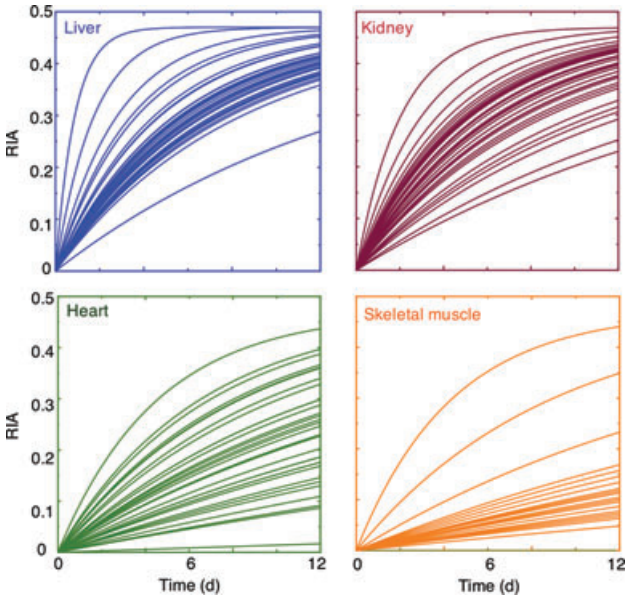

Figure 6. Turnover profiles for soluble proteins from four different mouse tissues. Temporal labelling profiles for proteins from four tissues (liver, kidney, heart and skeletal muscle) were obtained by in-gel digestion of protein spots followed by MALDI-TOF MS analysis of valine-containing peptides. For each tissue, the same spots ware excised, digested and subjected to MS to obtain the labelling profile for mono-valine peptides. Knowing the precursor pool RIA, it was then possible to calculate the first order rate profile for turnover of the protein. For this figure, the curves corresponding to the first order traces for the trajectory of (RIA, *t*) are plotted for ease of interpretation. The data for individual proteins are included in Supporting Information Fig. S1.

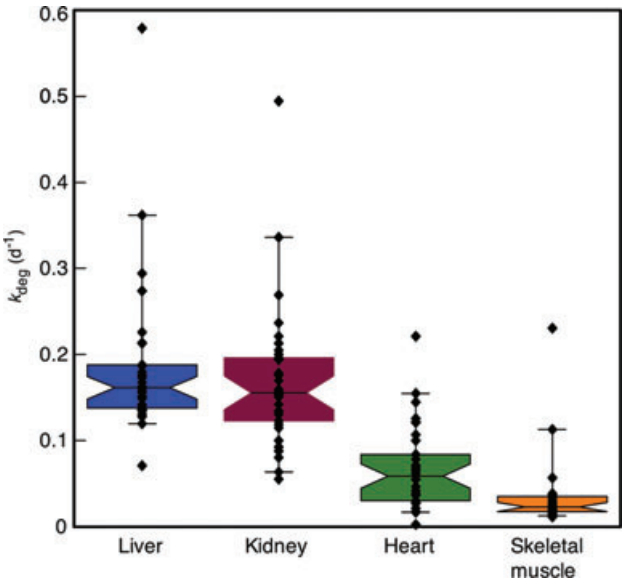

Figure 7. Comparison of turnover profiles for proteins in four different mouse tissues. For four tissues (liver, kidney, heart and skeletal muscle) the turnover profiles of between 22 (skeletal muscle) and 34 (liver, kidney, heart) proteins were obtained from MALDI-TOF MS analysis of spots cut from 2D-PAGE of soluble proteins, for duplicate animals at each of four time points over a 12-day period. The individual rate constants (diamonds, plotted in reciprocal time) are expressed as a notched box (median, half-width notch) and whiskers (5th and 95th percentile) plot.

reflecting lysosomal degradation by cathepsins or the 26S proteasome.

We have previously explored the turnover of one mouse muscle protein, glycogen phosphorylase (PYGM_MOUSE, Q9WUB3). This protein has a tightly bound cofactor, pyridoxal phosphate, derived from vitamin B6. In fact, about 50% of the vitamin B6 in the mouse is bound to this one protein. We have shown that the turnover of this protein can be accessed by stable isotope labelling with tritiated or deuterated pyridoxine, coupled with urinalysis of the metabolic dead-end product 4-pyridoxic acid [35, 36]. From the kinetics of vitamin B6 metabolism, we derived a degradation rate for glycogen phosphorylase of 0.09/day. In the analysis reported here, the same protein had a turnover rate of 0.06/day. However, the turnover rate of the muscle proteins was sufficiently low that isotope incorporation was limited, and would require labelling over an extended period to gain a more accurate turnover rate. Alternatively, the discrepancy between the two numbers could be taken as evidence of a slow but significant exchange of bound cofactor in vivo.

Although 2D-PAGE has somewhat fallen out of vogue in proteomics analyses, it should be reiterated that it remains the technique that has the highest resolution of protein separation methodologies, and is able to separate variants of proteins that differ by a single charge (e.g. that created by a deamidation event). For two proteins in heart and skeletal muscle, we were able to assess the kinetics of incorporation of deuterated valine into a series of spots on the gel representing charge variants of the same protein. If the different variants reflected a life-time dependent progression through different charge variants, it might be expected that the isotope abundance in different protein variants would differ, and the 'oldest' spots should have the lowest isotope incorporation. For beta-enolase (ENOB_MOUSE, P21550) and creatine kinase (KCRM_MOUSE, P07310), proteins that exist in multiple charge variants, we could detect no statistically significant difference in the RIA of valine (Fig. 9) and, thus, conclude that there is no evidence for age-dependent progression through the charge variants.

The deuterium present on the α-carbon atom of [$^2H_8$]valine is metabolically labile and known to exchange during transamination in vivo. Transamination is a rapidly reversible process, and, thus, will lead to the formation of valine in which the α-carbon deuterium atom will be replaced by an α-carbon hydrogen, which would be 7 Da heavier than unlabelled valine. Therefore, a 7 Da shift would be expected between peaks representing unlabelled and labelled peptides. During analysis of the mass spectra for labelled peptides, it was noticed that the peak corresponding to the labelled peptide did not

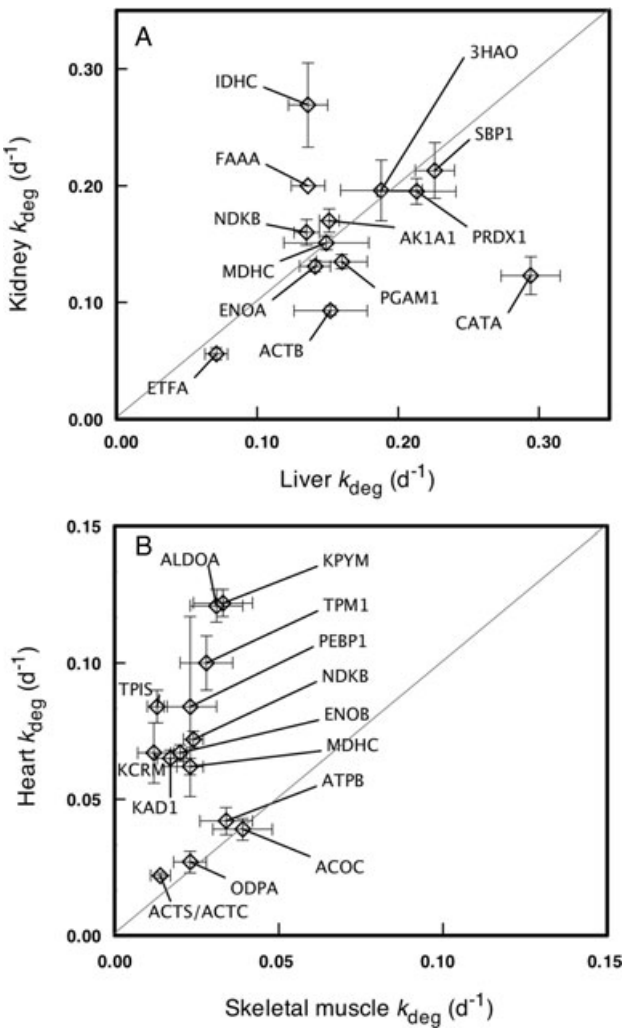

Figure 8. Tissue specific turnover rates. For a subset of proteins, turnover rates were determined in more than one tissue. The degradation rate constants (diamonds, ±SEM) were compared between high turnover tissues (liver, kidney) and low turnover tissues (skeletal muscle, heart). The diagonal line on each plot defines the line of equivalence.

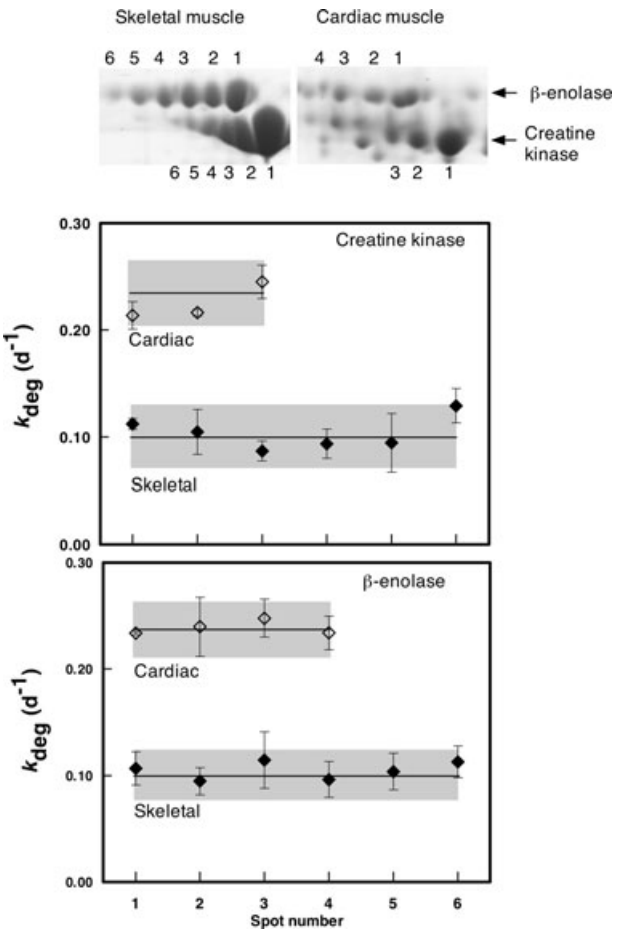

Figure 9. Turnover of resolvable isoforms of beta-enolase and creatine kinase in cardiac and skeletal muscle. Two proteins, creatine kinase and beta-enolase were both present in sufficiently high concentrations that 'charge trains' of spots were evident, and could be analysed for differences in turnover kinetics. For each protein, individual spots were digested from animals at day 12 and the RIA of isotope incorporation was obtained from monovaline peptides. For each protein/tissue the first order rate constant (±SEM) are plotted for each analysable spot, superimposed over these plots is the mean (line) and 95% confidence interval (shaded area) for the mean of the values for all spots discernible in one tissue/protein.

have the expected isotopomer envelope shape. Here both a 7 Da and an overlapping 8 Da shift were observed, producing a characteristic isotopomer envelope for labelled peptides, because the transamination process is incomplete. The +7 Da and +8 Da isotope envelopes are essentially identical and overlap by 1 Da such that the first ^{12}C peak of the 7 Da envelope has a lower intensity than would be expected for the natural isotope distribution, due to the additive effect of the +7 Da ^{13}C peak and the +8 Da ^{12}C peak (results not shown). The shape of the observed envelope can be used to calculate the percentage [$^{2}H_{7}$]valine present by comparing the predicted peak intensities for that specific peptide (calculated from the MS-Isotope tool) to those actually present in the mass spectrum. Fitting of the observed and predicted isotopic profile then reveals the degree of transamination of the amino acid. When this analysis was applied to both MUP and liver 'heavy' valine peptides, it was clear that there is a higher degree of transamination in the liver tissues than the MUPs (Fig. 10). This is most likely due to the rapid excretion of MUPs from the liver, so they are not accessible for transamination for as long as the amino acids derived from degradation of intrinsic liver proteins. Additionally, the retention of urine in the bladder between samplings could result in time-dependent pooling of MUPs between sampling, which could explain the variance in percentages calculated. The extent of transamination in heart and skeletal muscle was higher than liver, presumably reflecting the metabolic

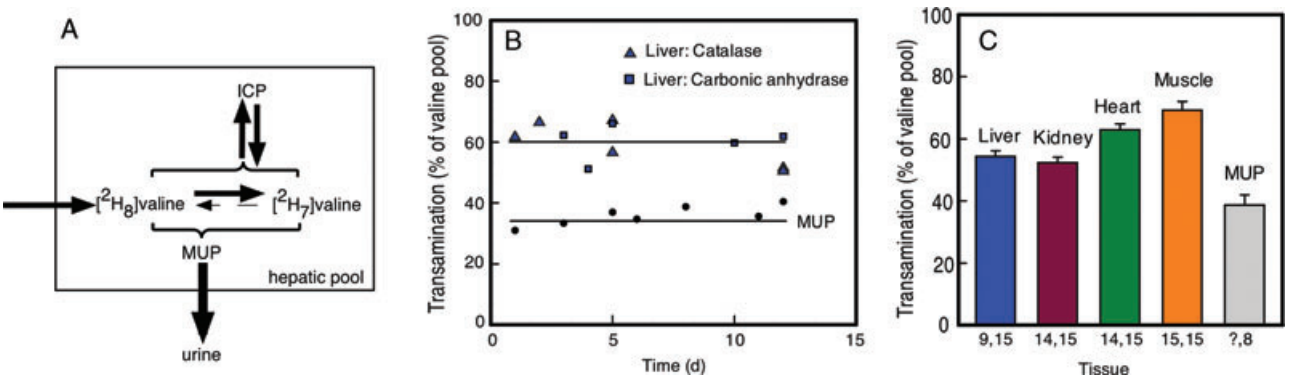

Figure 10. Comparison of valine transamination in different tissues. Although the ingested valine is octadeuterated ($[^2H_8]$), the liver, and possibly the small intestine, is capable of transamination of the amino acid, leading to loss of the α-deuteron (A). The complete isotope profile of the overlapping $[^2H_7]$ and $[^2H_8]$ profiles was analysed by non-linear curve fitting to recover the proportions of $[^2H_7]$ and $[^2H_8]$valine (see text). The extent of transamination of the amino acid in each protein or tissue could be determined. For liver, two ICP were analysed (catalase and carbonic anhydrase) as well as liver-synthesized MUPs, recovered from urine throughout the course of the labelling period (B). For the other tissues, similar data processing was conducted to derive the extent of transamination in different tissues at day 12 (C). For each of the tissues, the number of proteins and peptides contributing to the assessment of transamination (the histogram display is mean ± SEM) is given by the two numbers, in the format (proteins, peptides). For MUPs, it is not possible to define the number of proteins that contributed the peptides because of the extreme polymorphisms of this group of proteins; hence the '?'.

'distance' of these tissues from the liver pool and the higher residence time of the amino acid in these tissues.

4 Conclusions

The study of proteome dynamics requires detailed analysis of the kinetics of gain or loss of stable isotope labelled tracer into or from the proteome. In complex organisms, these are complex experiments requiring either uniformly labelled diets (such as those labelled with $[^{15}N]$) or diets in which specific amino acids are fully labelled by microbial incorporation of amino acids into protein. In the approach adopted here, we show that it is possible to monitor proteome dynamics by the simple expedient of supplementing existing standard laboratory diet with an equivalent quantity of stable isotope labelled valine. As we anticipated, there were differences in the rate of absorption of the free, stable isotope labelled amino acid and protein-bound unlabelled amino acid released through digestion. However, the frequency and amplitude of this variation was of little consequence relative to much lower rates of protein turnover. Moreover, all dietary administration to rodents incurs the probability of a diurnal variation in amino acid flux, as rodents only feed during the dark period. By using abundant secreted liver proteins that are subsequently excreted in urine (MUPs), it was possible to monitor this flux at a frequency that defined the oscillations, but for practical purposes this process would be intangible in most experimental designs. That being said, repeated monitoring of the MUPs offers a way to explore the high frequency component of the hepatic protein labelling curve. Moreover, the samples were obtained non-invasively, reducing the number of animals required for definition of the labelling trajectory. Of course, the urinary MUP profile can only report on the precursor pool behaviour in hepatic tissues. A protein secreted from kidney tissue such as meprin [37, 38] would be able to report on kidney protein synthesis, but precursor labelling trajectories in muscle and heart would be less accessible.

We also demonstrate that partial labelling of the diet is an entirely acceptable approach. The relative abundance of the stable isotope labelled amino acid reached the same value as that designed for the diet within a few days, and remained effectively stable for the reminder of the experiment. Because only a part of the precursor pool was labelled in this approach, it is necessary to measure the RIA of the precursor pool of protein synthesis using MIDA. The calculation of precursor RIA is facile and is arguably simpler in approach than detailed analysis of complex isotopomer profiles obtained from comprehensive atom centre labelling. The definition of this parameter need only be measured once for each tissue and can be recovered by analysis of peptides from abundant proteins, provided that they generate peptides that contain two or more instances of the labelled amino acid. Dietary labelling with an abundant amino acid, such as valine or leucine, increases the frequency of such peptides, as does peptide formation by an endopeptidase of greater specificity than trypsin, such as endopeptidase LysC. Once the RIA of the precursor pool is known, recovery of the replacement (= turnover) rate of each protein is straightforward.

In these studies, we used the lowest cost stable isotope labelled amino acid, specifically, a deuterated variant in which

all non-ionizable hydrogen atoms were replaced with deuterium. From previous work, we anticipated that the deuterium atom attached to the α-carbon atom would be lost through metabolism. In *Saccharomyces cerevisiae*, the loss of this atom is complete [17], but in animal systems, transamination of the amino acid pool is sufficiently slow that the valine was incorporated into protein as a mixture of [$^2H_7$] and [$^2H_8$]valine. The complex, overlapping isotopic profiles of the two components meant that analysis of the labelled peptides was not readily achieved by standard software packages, and for this study, we elected to analyse proteins resolved by 2D electrophoresis. This allowed us to explore the possibility that the 'charge-trains' commonly seen in 2D-PAGE reflected progressive ageing of the protein pool. We could discern no difference in the extent of labelling of the protein spots in the charge sequences, from which we infer that their interconversion must be much faster than the rate of turnover, and might indeed be reversible.

We believe it is possible to design relatively simple experimental workflows to assess proteome dynamics in intact animals. Simple supplementation of a standard diet with a stable isotope labelled essential amino acid that is present in the proteome at a high abundance, and which is deuterated at metabolically stable centres would create a relatively simple and low-cost workflow. Sampling of secreted/excreted protein would allow access to the kinetics of precursor pool labelling, and ensure optimal experimental design. Indeed, it might even be feasible to assess the turnover of tissue proteomes by analysis of urinary exosomes. As such approaches are simplified and designed, we should gain an increasing understanding of the proteome as a metabolically active entity in which both synthesis and degradation play a part in eliciting shifts in protein abundance – a true perspective on the 'dynamic proteome'.

We are grateful to Dr. Duncan Robertson for instrument support and to John Waters and Dr. Rick Humphries for animal care. This work was supported by EPSRC [grant EP/D013623/1] and NERC [grant NE/ G018650/1].

The authors have declared no conflict of interest.

5 References

[1] Schoenheimer, R., Rittenberg, D., Foster, G. L., Keston, A. S. et al., The application of the nitrogen isotope N15 for the study of protein metabolism. *Science* 1938, *88*, 599–600.

[2] Cargile, B. J., Bundy, J. L., Grunden, A. M., Stephenson, J. L. J., Synthesis/degradation ratio mass spectrometry for measuring relative dynamic protein turnover. *Anal. Chem.* 2004, *76*, 86–97.

[3] Price, J. C., Holmes, W. E., Li, K. W., Floreani, N. A. et al., Measurement of human plasma proteome dynamics with (2)H(2)O and liquid chromatography tandem mass spectrometry. *Anal. Biochem.* 2011, *420*, 73–83.

[4] Rachdaoui, N., Austin, L., Kramer, E., Previs, M. J. et al., Measuring proteome dynamics *in vivo*: as easy as adding water? *Mol. Cell Proteomics* 2009, *8*, 2653–2663.

[5] Hellerstein, M. K., Neese, R. A., Mass isotopomer distribution analysis at eight years: theoretical, analytic, and experimental considerations. *Am. J. Physiol.* 1999, *276*, E1146–E1170.

[6] Hellerstein, M. K., Neese, R. A., Mass isotopomer distribution analysis: a technique for measuring biosynthesis and turnover of polymers. *Am. J. Physiol.* 1992, *263*, E988–E1001.

[7] Papageorgopoulos, C., Caldwell, K., Shackleton, C., Schweingrubber, H. et al., Measuring protein synthesis by mass isotopomer distribution analysis (mida). *Anal. Biochem.* 1999, *267*, 1–16.

[8] Doherty, M. K., Hammond, D. E., Clague, M. J., Gaskell, S. J. et al., Turnover of the human proteome: determination of protein intracellular stability by dynamic silac. *J. Proteome. Res.* 2009, *8*, 104–112.

[9] Claydon, A. J., Beynon, R. J., Protein turnover methods in single-celled organisms: dynamic silac. *Methods Mol. Biol.* 2011, *759*, 179–195.

[10] Price, J. C., Guan, S., Burlingame, A., Prusiner, S. B. et al., Analysis of proteome dynamics in the mouse brain. *Proc. Natl. Acad. Sci. USA* 2010, *107*, 14508–14513.

[11] Schwanhausser, B., Gossen, M., Dittmar, G., Selbach, M., Global analysis of cellular protein translation by pulsed silac. *Proteomics* 2009, *9*, 205–209.

[12] Beynon, R. J., Pratt, J. M., Strategies for measuring dynamics: the temporal component of proteomics. *Methods Biochem. Anal.* 2006, *49*, 15–25.

[13] Doherty, M. K., Beynon, R. J., Protein turnover on the scale of the proteome. *Expert Rev. Proteomics* 2006, *3*, 97–110.

[14] Hayter, J. R., Doherty, M. K., Whitehead, C., McCormack, H. et al., The subunit structure and dynamics of the 20s proteasome in chicken skeletal muscle. *Mol. Cell Proteomics* 2005, *4*, 1370–1381.

[15] Beynon, R. J., Pratt, J. M., Metabolic labeling of proteins for proteomics. *Mol. Cell Proteomics* 2005, *4*, 857–872.

[16] Doherty, M. K., Whitehead, C., McCormack, H., Gaskell, S. J. et al., Proteome dynamics in complex organisms: using stable isotopes to monitor individual protein turnover rates. *Proteomics* 2005, *5*, 522–533.

[17] Pratt, J. M., Petty, J., Riba-Garcia, I., Robertson, D. H. et al., Dynamics of protein turnover, a missing dimension in proteomics. *Mol. Cell Proteomics* 2002, *1*, 579–591.

[18] Zhang, Y., Reckow, S., Webhofer, C., Boehme, M. et al., Proteome scale turnover analysis in live animals using stable isotope metabolic labeling. *Anal. Chem.* 2011, *85*, 1665–1672.

[19] Kruger, M., Moser, M., Ussar, S., Thievessen, I. et al., Silac mouse for quantitative proteomics uncovers kindlin-3 as an essential factor for red blood cell function. *Cell* 2008, *134*, 353–364.

[20] Albaum, S. P., Hahne, H., Otto, A., Haussmann, U. et al., A guide through the computational analysis of isotope-labeled mass spectrometry-based quantitative proteomics data: an

application study. *Proteome Sci.* 2011, *9*, 30.

[21] Guan, S., Price, J. C., Prusiner, S. B., Ghaemmaghami, S. et al., A data processing pipeline for mammalian proteome dynamics studies using stable isotope metabolic labeling. *Mol. Cell Proteomics* 2011, doi: 10.1074/mcp.M111.010728.

[22] Hoopmann, M. R., Chavez, J. D., Bruce, J. E., Silactor: software to enable dynamic silac studies. *Anal. Chem.* 2011, *83*, 8403–8410.

[23] Haegler, K., Mueller, N. S., Maccarrone, G., Hunyadi-Gulyas, E. et al., Quantispec–quantitative mass spectrometry data analysis of (15)N-metabolically labeled proteins. *J. Proteomics* 2009, *71*, 601–608.

[24] Busch, R., Kim, Y. K., Neese, R. A., Schade-Serin, V. et al., Measurement of protein turnover rates by heavy water labeling of nonessential amino acids. *Biochim. Biophys. Acta* 2006, *1760*, 730–744.

[25] Iresjo, B. M., Svanberg, E., Lundholm, K., Reevaluation of amino acid stimulation of protein synthesis in murine- and human-derived skeletal muscle cells assessed by independent techniques. *Am. J. Physiol. Endocrinol. Metab.* 2005, *288*, E1028– E1037.

[26] Roberts, S. A., Simpson, D. M., Armstrong, S. D., Davidson, A. J. et al., Darcin: a male pheromone that stimulates female memory and sexual attraction to an individual male's odour. *BMC Biol.* 2010, *8*, 75.

[27] Cheetham, S. A., Smith, A. L., Armstrong, S. D., Beynon, R. J. et al., Limited variation in the major urinary proteins of laboratory mice. *Physiol. Behav.* 2009, *96*, 253–261.

[28] Armstrong, S. D., Robertson, D. H., Cheetham, S. A., Hurst, J. L. et al., Structural and functional differences in isoforms of mouse major urinary proteins: a male-specific protein that preferentially binds a male pheromone. *Biochem. J.* 2005, *391*, 343–350.

[29] Beynon, R. J., Hurst, J. L., Urinary proteins and the modulation of chemical scents in mice and rats. *Peptides* 2004, *25*, 1553–1563.

[30] Hurst, J. L., Beynon, R. J., Scent wars: the chemobiology of competitive signalling in mice. *Bioessays.* 2004, *26*, 1288–1298.

[31] Beynon, R. J., Veggerby, C., Payne, C. E., Robertson, D. H. et al., Polymorphism in major urinary proteins: molecular heterogeneity in a wild mouse population. *J. Chem. Ecol.* 2002, *28*, 1429–1446.

[32] Hurst, J. L., Payne, C. E., Nevison, C. M., Marie, A. D. et al., Individual recognition in mice mediated by major urinary proteins. *Nature* 2001, *414*, 631–634.

[33] Kim, J., Kim, J. I., Jang, H. S., Park, J. W. et al., Protective role of cytosolic $NADP^+$-dependent isocitrate dehydrogenase, IDH1, in ischemic pre-conditioned kidney in mice. *Free Radic. Res.* 2011, *45*, 759–766.

[34] Kim, J., Kim, K. Y., Jang, H. S., Yoshida, T. et al., Role of cytosolic $NADP^+$-dependent isocitrate dehydrogenase in ischemia-reperfusion injury in mouse kidney. *Am. J. Physiol. Renal. Physiol.* 2009, *296*, F622–F633.

[35] Beynon, R. J., Leyland, D. M., Evershed, R. P., Edwards, R. H. et al., Measurement of the turnover of glycogen phosphorylase by GC/MS using stable isotope derivatives of pyridoxine (vitamin B6). *Biochem. J.* 1996, *317*, 613–619.

[36] Leyland, D. M., Beynon, R. J., The expression of glycogen phosphorylase in normal and dystrophic muscle. *Biochem. J.* 1991, *278*, 113–117.

[37] Jiang, W., Gorbea, C. M., Flannery, A. V., Beynon, R. J. et al., The alpha subunit of meprin A. Molecular cloning and sequencing, differential expression in inbred mouse strains, and evidence for divergent evolution of the alpha and beta subunits. *J. Biol. Chem.* 1992, *267*, 9185–9193.

[38] Beynon, R. J., Oliver, S., Robertson, D. H., Characterization of the soluble, secreted form of urinary meprin. *Biochem. J.* 1996, *315*, 461–465.

